THEORETICAL & APPLIED MECHANICS LETTERS **1**, 011007 (2011)

Influence of precipitation on the Portevin-Le Chatelier effect in Al-Mg alloys

Qi Hu,[a] Qingchuan Zhang,[b] Shihua Fu, Pengtao Cao, and Ming Gong
CAS Key Laboratory of Mechanical Behavior and Design of Materials, University of Science and Technology of China, Hefei 230027, China

(Received 20 October 2010; accepted 23 November 2010; published online 10 January 2011)

Abstract In the alloy with solute content higher than the limiting solubility, the solute atoms that have failed to dissolve will precipitate from the solid solution and form precipitations. In this study, the Portevin-Le Chatelier (PLC) effects in annealed 5456 and 5052 aluminum alloys with different precipitation contents have been investigated under different applied strain rates. The results suggest that precipitations have significant effect on the PLC effect and the more the precipitations are, the greater the influence is. Furthermore, the solute diffusion is pipe diffusion in 5052 alloy with lower precipitation content. However, for 5456 alloy with higher precipitation content, the diffusion is no longer the case but more complex. © *2011 The Chinese Society of Theoretical and Applied Mechanics.* [doi:10.1063/2.1101107]

Keywords aluminum alloys, Portevin–Le Chatelier effect, dynamic strain aging, tension test

An irregular unstable plastic flow, which manifests itself as temporal continuous serrated yielding on stress–strain curves and repeated spatial propagation of strain localization, can be observed macroscopically in many metal alloys in various tests (including tension, compression, torsion, etc.) within a certain range of temperatures and strain rates. The phenomenon is commonly referred to as Portevin-Le Chatelier (PLC) effect.[1,2] The spatial strain localizations are usually in the form of deformation bands and can be qualitatively categorized into three "types" by diverse spatial propagation and serration characteristics.[3−7] Type A deformation band continuously propagates along the traction axis under a higher strain rate or lower temperature,[4] and the serrations on stress versus strain curves are indistinct and hard to identify. Type B band nucleates in the direction of traction axis under a medium strain rate or temperature, and propagates in a hopping manner. The serrations are distinct and relatively regular, vibrating around the envelope curve. Under a lower strain rate or higher temperature, type C band no longer exhibits propagation characteristics and stochastically nucleates on the specimen surface. The serrations are quite obvious and below the envelope curve usually.[7]

It is widely accepted that the physical origin of PLC effect is known to arise from a micro structural process denoted by Dynamic Strain Aging (DSA),[8] namely, the dynamic interaction between mobile dislocations and solute atoms. On the microscopic scale, the motion of mobile dislocation is intermittent and can be impeded by obstacles such as forest dislocations and grain boundaries etc. As a sort of line defect in crystal, mobile dislocation will cause lattice deformation around it and generate a stress field. Solute atoms will cluster by diffusion under the action of stress filed during an appropriate range of temperature and strain rate. A solute cloud may form and the mobile dislocation will be effectively pinned. With applied stress, obstacles can be conquered by thermally activated dislocation motion. This unpinning process of dislocation may cause a stress drop on the macroscopic stress curve. Therefore, the PLC effect is in response to the dynamic repeated pinning and unpinning processes between mobile dislocations and solute atoms.

Due to the controversy about the special mechanism on DSA, extensive experimental and theoretical research has been carried out based on different understandings.[9−14] However, this research mostly focuses on the interaction between solute atoms and defects in crystal (such as forest dislocations, grain boundaries etc.). More and more research indicates that precipitations play an important role in the PLC effect and have an effect on its appearance and evolution. Especially in alloys with solute content higher than the limiting solubility, a large number of precipitations precipitate from the solid solution and lead to lattice deformation, which increases the impediment to the motion of dislocations.[15,16] In Sun *et al.*,[17] we have investigated the influence of precipitations on the PLC effect in an Al-Cu alloy by solution treatment at different temperatures, and found that precipitations have a remarkable effect on the PLC effect in alloy with relatively higher precipitation content when the solution treatment temperature is lower than 300 °C.

In this paper, the influences of different precipitation contents on the PLC effect in Al-Mg alloys under different applied strain rates were investigated by the analysis on the characteristic parameters such as the critical strain, the stress drop amplitude etc.

The materials studied in this paper are the aluminum alloy 5456 and 5052. The chemical composition (in wt. %) is Al-5Mg-0.1Cu-0.5Mn-0.4Fe-0.25Si-0.25Zn-0.1Cr for 5456 alloy and Al-2.5Mg-0.1Cu-0.1Mn-0.4Fe-0.25Si-0.1Zn-0.15Cr for 5052 alloy respectively.

Before heat processing, specimens with a gauge

[a] E-mail: huqi2007@mail.ustc.edu.cn
[b] Corresponding author. E-mail: zhangqc@ustc.edu.cn.

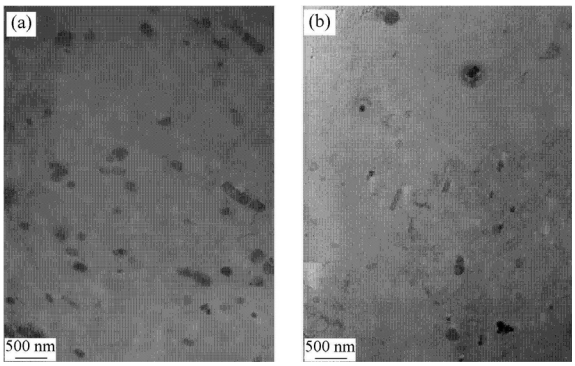

Fig. 1. TEM images of precipitations obtained after the heat treatments. (a) 5456 alloy; (b) 5052 alloy.

of 55 mm×20 mm×3 mm were cut from a 3 mm-thick plate along the rolling direction. The specimens were annealed at 673 K for 3h and then furnace cooled to ambient temperature before tension. Specimens were deformed in a special tensile machine with crosshead speeds of 20, 15, 7.2, 1.8 and 0.6 mm/min at room temperature. The corresponding nominal strain rates are 6.1×10^{-3}, 4.5×10^{-3}, 2.2×10^{-3}, 5.5×10^{-4} and $1.8\times10^{-4}\,s^{-1}$ respectively. The load and the displacement were recorded during tension and the sampling frequency was selected from 25 Hz to 100 Hz according to the applied strain rates. The micro-structure of alloys, especially the size and the distribution of precipitations, were examined employing a JEOL-2011 transmission electron microscope (TEM).

The Mg solute contents in the investigated materials 5456 and 5052 are 5% and 2.5% respectively. But the theoretical solubility of Mg is less than 1% at room temperature.[18] Thus, the Mg solute failed to dissolve in Al will form precipitations (such as Mg_5Al_8, Mg_2Si etc.) The concentration of solute atoms dissolved in Al can be considered equivalent for the two investigated alloys at room temperature. Therefore, the difference in mechanical properties for the two alloys should result from the different precipitation contents.

The TEM images for the annealed 5456 and 5052 aluminum alloys are shown in Fig. 1. It can be seen that the size and the distribution of precipitations are different within both investigated materials. For 5456 alloy (Fig. 1(a)), the precipitations are concentrated and distribute evenly. The precipitations of tens to hundreds of nanometers can be observed. But, the precipitation content is lower for 5052 alloy and the particles distribute sparsely (Fig. 1(b)). The size of precipitation is relatively greater and of hundreds of nanometers. It can be observed from Fig. 1 that the precipitation content increases with the Mg solute content.

Figure 2 shows the stress versus strain curves under different applied strain rates for the two annealed alloys. The stress and the strain in this paper refer to the nominal stress and the nominal strain respectively.

In Fig. 2, it can be observed that the whole feature of tension curves and the morphology of local ser-

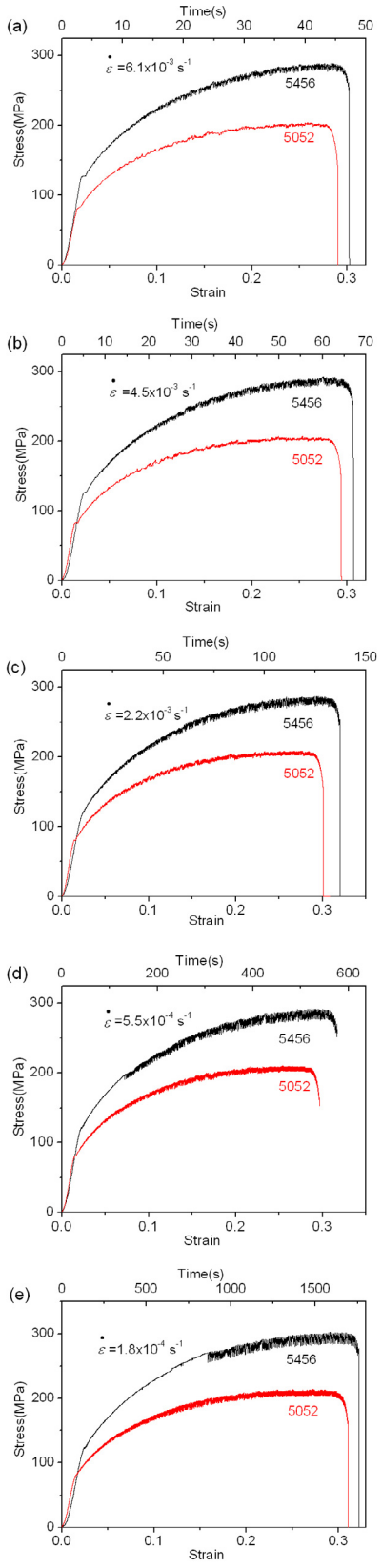

Fig. 2. Stress versus strain curves under different applied strain rates for the two annealed alloys. The upper axis represents the corresponding time. (a) $6.1\times10^{-3}\,s^{-1}$; (b) $4.5\times10^{-3}\,s^{-1}$; (c) $2.2\times10^{-3}\,s^{-1}$; (d) $5.5\times10^{-4}\,s^{-1}$; (e) $1.8\times10^{-4}\,s^{-1}$.

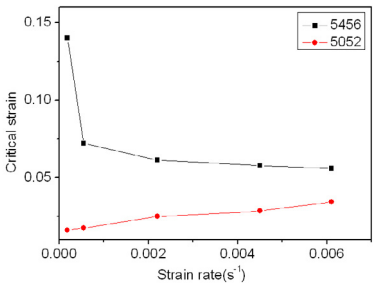

Fig. 3. The dependence of critical strain on the strain rate.

rations show great differences under different applied strain rates for the two alloys. With the applied strain rate decreasing, the serration type changes from type B to type C for 5456 alloy and from type A to type B for 5052 alloy. The strength, the ductility and the drop amplitude of serration increase with the Mg solute content under the same applied strain rate. More precipitations lead to more impediments to the motion of dislocations and more dispersion strengthening during plastic deformation. Thus, the yield strength and fracture strength are higher for 5456 alloy. Similarly, the mobile dislocations need more energy to be accumulated for conquering the impediments from the precipitations, which leads to the higher stress drop amplitudes. This indicates that precipitations play an important role in the PLC effect.

Figure 3 shows the dependence of critical strain for the onset of PLC effect on the strain rate for the two alloys. The critical strain shows different evolution with strain rate. For 5456 alloy, the critical strain decreases with strain rate (behavior called "abnormal") and the evolution is similar to an exponential decay. However, the critical strain linearly increases with strain rate for 5052 alloy (behavior called "normal"). For 5456 alloy with more precipitations, the dislocation motion becomes gradually slower with decreasing strain rate. A large number of precipitations lead to more impediments to the motion of dislocations. The mobile dislocations need more time to accumulate energy for conquering the impediments, which gives rise to the "abnormal" characteristic. However, the impediments to the dislocations are inconspicuous due to the lower precipitations in 5052 alloy. It is hard for the solute atoms to form a solute cloud around the dislocation and to pin it effectively due to the high glide speed of dislocations. More time will be demanded for the forest dislocation density to increase adequately to slow down the mobile dislocation motion and then the DSA occurs, which gives rise to the "normal" characteristic.

Figures 4(a) and (b) show the average drop amplitude versus strain rate curves for the two alloys in a certain range of strain (6%–8%, 12%–14%, 18%–20%). The average drop amplitude decreases with strain rate and exhibits negative strain rate sensitivity (NSRS) obviously. Both of them exhibit a tendency of exponential

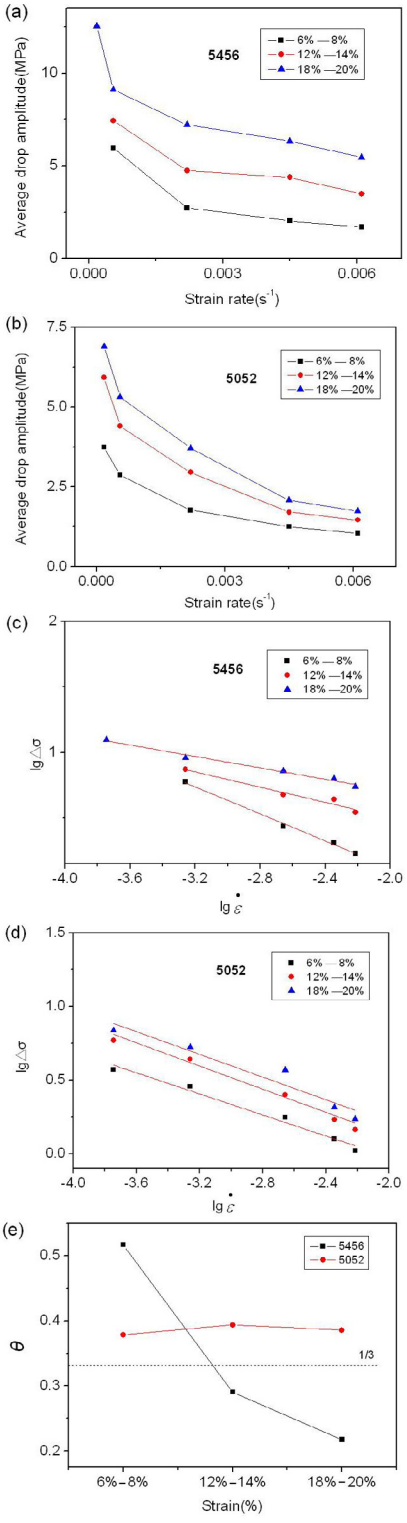

Fig. 4. The evolution of average drop amplitude with strain rate in a certain range of strain (6%–8%, 12%–14%, 18%–20%) respectively. (a) The dependence of average drop amplitude on the strain rate for 5456 alloy; (b) The dependence of average drop amplitude on the strain rate for 5052 alloy; (c) The dependence of logarithmic average drop amplitude on the logarithmic strain rate for 5456 alloy; (d) The dependence of logarithmic average drop amplitude on the logarithmic strain rate for 5052 alloy; (e) The evolution of exponent θ with strain.

decay and can be expressed approximately by

$$\Delta\sigma \propto k\dot{\varepsilon}^{-\theta}. \tag{1}$$

Furthermore, the dependence of the logarithm of the average drop amplitude on the logarithm of the strain rate for the two alloys has been shown in Fig. 4(c) and (d) respectively. The logarithm of the average drop amplitude decreases linearly with the logarithm of the strain rate. Thus, the slope is the exponent $-\theta$ according to the expression (1). From Fig. 4(c) and (d), the relation between the exponent θ and the strain has been obtained as shown in Fig. 4(e). The exponent θ decreases with strain from 0.52 to 0.22 for 5456 alloy, but it keeps constant, approximately 1/3, for 5052 alloy.

The applied strain rate $\dot{\varepsilon}$ is supposed to be inversely proportional to the waiting time $t_{\rm w}$, the time for mobile dislocations waiting to be thermally activated before the obstacles[19]

$$\dot{\varepsilon} = \frac{\Omega}{t_{\rm w}}, \tag{2}$$

where Ω is a strain increment produced when all arrested dislocations overcome localized obstacles and advance to the next pinned configuration. So

$$\Delta\sigma \propto at_{\rm w}^{\theta}. \tag{3}$$

The PLC effect is in response to the dynamic repeated pinning and unpinning processes between mobile dislocations and solute atoms according to the DSA. So the pinning strength, namely, the stress drop amplitude is in connection with the solute concentration around the dislocation. According to the Cottrell-Bilby type kinetics, the solute concentration around the dislocation can be expressed by[20]

$$c_{\rm s} = c_{\rm m}[1 - \exp(-pt^{\theta})], \tag{4}$$

where $c_{\rm s}$ is the solute concentration, $c_{\rm m}$ is the saturation, t is the effective time for the solute diffusing to the dislocation, namely, the waiting time $t_{\rm w}$, and p is a constant concerned with the solute diffusion. θ is a constant and $\theta = 1/3$ for pipe diffusion or $\theta = 2/3$ for bulk diffusion. In this paper, θ is different for the two investigated alloys according to the experimental data. It is approximately 1/3 for 5052 alloy, which is in accordance with the result in McCormick.[20] It indicates that the solute atoms form atmosphere around the dislocations by pipe diffusion when the mobile dislocations have been impeded by obstacles. However, it is not the case for 5456 alloy due to the change in θ. The precipitations in 5456 alloy are much more than those in 5052 alloy. In the case of same conditions for the two alloys, it can be concluded that the formation of solute atmosphere is more complex in 5456 alloy because more precipitations participate in the DSA and impede the motion of mobile dislocations. The special diffusion mechanism for 5456 alloy, as mentioned above, need to be further investigated in the future.

In the present article, the PLC effect in the two annealed Al-Mg alloys with different precipitation contents have been investigated under different applied strain rates. The following conclusions can be drawn from the present study: (1) In the DSA theory giving rise to the PLC effect, the mobile dislocation will be impeded not only by the obstacles (such as the forest dislocations and grain boundaries etc.), but also by the precipitations. A large number of precipitations increase the impediments to the motion of mobile dislocations, and play an important role in the PLC effect. (2) The more the precipitations are, the greater the influence on the PLC effect is. (3) The solute atoms diffuse to dislocation by pipe diffusion in 5052 alloy and the exponent $\theta = 1/3$ approximately. However, the diffusion is more complex in 5456 alloy due to the change in the exponent θ. It can be concluded that more precipitations participate in the DSA and make the diffusion more complex.

The financial support received from the National Natural Science Foundation of China under Grant Nos. 10732080, 10872189 is gratefully acknowledged.

1. A. Portevin and F. Le Chatelier, Comp. Rend. Acad. Sci. **176**, 507 (1923).
2. R. A. Mulford and U. F. Kocks, Acta Metall. **27**, 1125 (1979).
3. E. Pink and A. Grinberg, Mater. Sci. Eng. A **51**, 1 (1981).
4. M. Lebyodkin, L. Dunin-Barkovskii, Y. Bréchet, Y. Estrin, and L. Kubin, Acta Mater. **48**, 2529 (2000).
5. K. Chihab, Y. Estrin, L. P. Kubin, and J. Vergnol, Scrip. Metall. **21**, 203 (1987).
6. Q. C. Zhang, Z. Y. Jiang, H. F. Jiang, Z. J. Chen, and X. P. Wu, Int. J. Plasticity **21**, 2150 (2005).
7. T. A. Lebedkina and M. A. Lebyodkin, Acta Mater. **56**, 5567 (2008).
8. A. H. Cottrell, *Dislocations and Plastic Flow in Crystals*. (Oxford University Press, 1953).
9. Y. Estrin and L. P. Kubin, Acta Metall. **34**, 2455 (1986).
10. G. Ananthakrishna and D. Sahoo, J. Phys D: Appl. Phys. **14**, 2081 (1981).
11. E. Rizzi and P. Hähner, Int. J. Plasticity **20**, 121 (2004).
12. H. F. Jiang, Q. C. Zhang, X. D. Chen and, Z. J. Chen, Acta Mater. **55**, 2219 (2007).
13. W. Tong, H. Tao, N. Zhang, and Jr. L. G. Hector, Scr. Mater. **53**, 87 (2005).
14. A. Benallal, T. Berstad, T. Børvik, O. S. Hopperstad, I. Koutiri, and R. Nogueira de Codes, Int. J. Plasticity **24**, 1916 (2008).
15. Y. Brechet and Y. Estrin, Acta Metall. **43**, 955 (1995).
16. D. Thevenet, M. Mliha-Touati and A. Zeghloul, Mater. Sci. Eng. A. **266**, 175 (1999).
17. L. Sun, Q. C. Zhang and P. T. Cao, Chinese Physics B **18**, 3500 (2009).
18. J. L. Murray, Bulletin of Alloy Phase Diagrams **3**, 60 (1982).
19. S. Zhang, P. G. McCormick, and Y. Estrin, Acta Metall. **49**, 1087 (2001).
20. P. G. McCormick and C. P. Ling, Acta Metall. **43**, 1969 (1995).